

# GASLIGHT: Gaussian Splats for Spatially-Varying Lighting in HDR

Christophe Bolduc<sup>1</sup> Yannick Hold-Geoffroy<sup>2</sup> Zhixin Shu<sup>2</sup> Jean-François Lalonde<sup>1</sup>  
<sup>1</sup>Université Laval, <sup>2</sup>Adobe



Figure 1. We introduce GASLIGHT, a framework that captures environment lighting as HDR Gaussian Splats. From a sequence of regular photographs of a scene (backgrounds), GASLIGHT generates plausible illumination and can readily be applied as lighting in a 3D renderer to composite virtual objects onto images. Our representation inherently provides both high-frequency texture for reflections, as shown in the mirror sphere, and plausible light intensity, as seen in the shading of the inserted spheres and torus.

## Abstract

We present GASLIGHT, a method that generates spatially-varying lighting from regular images. Our method proposes using HDR Gaussian Splats as light source representation, marking the first time regular images can serve as light sources in a 3D renderer. Our two-stage process first enhances the dynamic range of images plausibly and accurately by leveraging the priors embedded in diffusion models. Next, we employ Gaussian Splats to model 3D lighting, achieving spatially variant lighting. Our approach yields state-of-the-art results on HDR estimations and their applications in illuminating virtual objects and scenes. To facilitate the benchmarking of images as light sources, we introduce a novel dataset of calibrated and unsaturated HDR to evaluate images as light sources. We assess our method using a combination of this novel dataset and an existing dataset from the literature. The code to reproduce our method will be available upon acceptance.

## 1. Introduction

Lighting is crucial not just for shaping an image, but also for ensuring realism and aesthetic appeal when inserting virtual content. Estimating accurate lighting representations from one or many photographs is vital for creating lifelike visuals that convincingly blend within their surroundings and con-

vey realistic surface appearance. This is essential in numerous applications including multimedia productions, virtual reality, forensics, cultural displays, and more.

Despite its importance, current methods face significant limitations in capturing and representing lighting accurately. One reason for this is the difficulty in capturing high dynamic range (HDR), which require multiple exposures [10] or specialized apparatus [41, 58]. Most approaches [12, 36, 69] therefore attempt to convert regular, low-dynamic range (LDR) images to HDR. However, as will be demonstrated later, they primarily focus on extending the dynamic range for tonemapping and visualization purposes [20, 24, 62], rather than extrapolating the intensity of bright light sources.

Another reason is the difficulty of simultaneously estimating HDR lighting that is both spatially-varying and high frequency. Tab. 1 provides an overview of existing lighting representations that have been proposed in the literature. Existing approaches either focus on accurate energy estimation, using parametric light sources [17], which allow for near-field effects, such as positioning a discrete lamp in the scene. Alternatively, per-pixel spherical harmonics [18] or tend to struggle in modeling high-frequency lighting and cannot generate strong cast shadows. Volumetric representations [32, 33, 57, 66] do not accurately model high-frequency lighting variations, as needed for reflections on glossy surfaces and do not readily integrate within ex-

	Param.	SH	Vol.	IBL	Ours
Near-field	✓	✗	✓	✗	✓
Spatially-varying	✓	✓	✓	✗	✓
HF reflections	✗	✗	✗	✓	✓
HF lighting	✓	✗	✓	✓	✓
Easy	✓	✓	✗	✓	✓

Schematic

Table 1. Comparison of different lighting representations. We include parametric (point or directional light sources, “param.”), Spherical Harmonics (“SH”), volumetric (“Vol.”), environment maps (“IBL”), and our proposed HDR GS representation. Aspects compared are near-field effects, such as the ability to represent a light source *within* the scene, High-Frequency reflections allowing for high-resolution details in reflections, High-Frequency lighting allowing strong shadows, and its overall ease of use (*e.g.*, integration in existing rendering engines).

isting rendering engine. Another prevalent representation used by lighting estimation methods is the environment map [9, 16, 44, 55, 56] (commonly referred to as IBL, for image-based lighting), which models infinitely-distant lighting as a spherical image. This representation cannot yield near-field lighting effects, such as a lamp in the scene, and model lighting as an infinitely-distant sphere. These limitations reduce the versatility of current lighting estimation methods, impacting their ability to achieve realistic lighting in scenes.

In this work, we introduce GASLIGHT, a novel method that addresses these challenges by capturing the high-frequency and spatially-varying lighting of a scene. It allows for near-field lighting effects, and readily integrates within existing rendering engines. GASLIGHT employs HDR Gaussian Splats as light representation, which is reconstructed from a set of LDR images. As opposed to HDRGS [6] (or HDR-NeRF [27]), our approach does not require alternating exposures to recover the HDR—rather we rely on a novel, specially-designed LDR-to-HDR network based on powerful diffusion models. Compared to previous NeRF-based HDR estimation approaches [19], our method is more accurate, does not require per-scene finetuning, and is much faster.

In summary, our contributions are threefold. First, we present a **framework for using Gaussian Splats as a spatially-varying HDR light representation** that can be estimated from a few images of a scene. This light representation can readily be used in a 3D renderer, enabling accurate and versatile lighting effects. Second, at the heart of our framework is a novel **LDR-to-HDR estimation model**, which leverages the strong priors in diffusion models to plausibly estimate the intensity of light sources. Finally, we **compare our method on existing HDR datasets from the literature**, and show that our methods best predicts the

intensity of bright light sources. We also demonstrate its applicability for virtual object insertion where virtual objects can be inserted at multiple locations in the scene and relit appropriately in a multi-view setting.

## 2. Related work

**Inverse tonemapping** has been an active area of research for several decades, with early methods focusing on inverting the camera function through various ad-hoc extrapolation techniques [1, 25]. Later, this topic was revisited using deep learning, first using end-to-end approaches [12, 13, 37], then by explicitly inverting the camera pipeline [36]. Inverse tonemapping has also been applied to spherical 360° panoramas, both outdoors [72] and indoors [69].

More recently, generative imaging has been utilized in inverse tonemapping, with GlowGAN [60] being the first to recover a multi-exposure bracket, as in traditional HDR capture [10]. Exposure Diffusion [3] improves this idea by adding exposure constraints to a pretrained diffusion model to generate relative exposures. While it capitalizes on the robust priors found in diffusion models, this method is restricted to pixel-space diffusion. Subsequently, LeDiff [62] finetunes a latent diffusion model [50] to determine relative exposures and merge them into an image with an extended dynamic range. Although this method shows promising results with latent-space diffusion for inverse tonemapping, it remains constrained by the decoder’s restricted dynamic range, which does not fully represent the richness of natural lighting. Our method draws inspiration from recent diffusion-based HDR estimation to propose an iterative dynamic range expansion scheme, enabling a significantly greater increase in dynamic range than current approaches allow.

**3D scene representations** The way 3D content is represented has evolved significantly over time, addressing different aspects such as geometry and appearance. Traditional methods often relied on textured 3D meshes [15] as the primary means to represent scene geometry and appearance. Implicit radiance functions, such as those introduced in Neural Radiance Fields (NeRFs) [38], have revolutionized 3D scene representations by leveraging neural networks to represent complex geometries and appearances, successfully modeling complex, view-dependent effects. HDR-NeRF [27], HDR-HexPlane [68], and others [28, 39, 65] have extended this framework to handle HDR content, allowing for the reconstruction of scenes with an extended dynamic range. PanoHDR-NeRF [19] combine an LDR-to-HDR network trained for 360° panoramas with an omnidirectional NeRF representation to capture the spatially-varying HDR light field of an indoor scene.

Later, explicit radiance functions based on 3D Gaussian Splatting [29] were proposed. HDR-GS [6] and

CineGR [61], leveraged multi-exposure input photographs to capture an extended dynamic range, similarly to their predecessor HDR-NeRF. As opposed to these methods, we focus on the extrapolation of the bright light sources present in the scene and do so without the requirement of multi-exposure inputs. We therefore create an explicit GS-based HDR representation, allowing them to function effectively as light sources for 3D renderers.

**Camera pose estimation** To capture scenes in the wild, a common first step is to estimate the relative camera pose between pictures taken of a given scene. The classical way to achieve this is through bundle adjustment [59], a method which has been revisited recently by COLMAP [52, 53]. Through time, classical feature descriptors used for matching made way to learned descriptors [11, 51], which evolved to end-to-end learned relative camera pose estimation methods such as Mickey [2], Dust3r [64] and its follow-up, Mast3r [31]. We encourage the reading of the survey provided in [63].

**Lighting representations** have evolved significantly over time, each addressing different aspects of light modeling and scene illumination. Parametric lights, such as point lights or directional lights, have been foundational since the inception of computer graphics. Methods that learn to predict parametric lights from images have been proposed [17, 22, 71], providing intuitive control over lighting but often struggle with accurately representing complex environments.

Spherical harmonics offer an efficient representation for lighting in real-time applications. They have been used to model both irradiance [21, 47] and radiance [54]. Garon et al. [18] estimate spatially-varying spherical harmonics directly from a single image.

Environment maps [4] provide a non-parametric alternative for capturing complex lighting environments, as they represent an infinitely distant light source modeled as a spherical image. They have been employed in many lighting estimation methods [9, 16, 19, 26, 44, 55, 56]. Implicit volumetric lighting representations were also devised to model both indoor [33, 57] and outdoor [67] lights, or for inverse rendering purposes [34]. Their opaqueness thwarts their powerful modeling capabilities, making them challenging to interpret and edit. In contrast, using Gaussian splats as a lighting representation combines the strengths of both parametric and non-parametric approaches. By representing HDR Gaussians with light-emitting spherical harmonics, our method provides spatially-varying lighting capabilities while maintaining the flexibility and interpretability of parametric representations.

### 3. Method

Our method takes a set of regular LDR images as input and produces lighting as an HDR 3D Gaussian Splats (3DGS) scene. The 3DGS can then be queried to obtain the amount of incoming radiance from a specific direction for rendering purposes. We break down our method into two steps. First, we uplift the LDR image to unsaturated HDR, providing plausible intensities for the observed light sources. Then, we fit the 3DGS scene to the estimated HDR content. It is important to note that our method does not perform lighting estimation from unseen parts of the scene—rather, it models only the lights visible within at least one image. We first describe our per-image light intensity estimation method, followed by the 3D scene reconstruction we employ.

#### 3.1. HDR light intensity estimation

Our HDR estimation method aims to produce a plausible hallucination of the intensities of the bright light sources present in an LDR image. As illustrated in fig. 2, our approach relies on a diffusion model  $\mathcal{D}$ , which accepts as input an image at a certain exposure  $I_0$ , and is trained (fig. 2a) to predict two versions of the input image at different exposures:  $I_{-2} = \mathcal{D}_-(I_0)$ , and  $I_{+2} = \mathcal{D}_+(I_0)$ . Here, the  $I_X$  notation means applying a  $2^X$  factor to the exposure of the input image  $I_0$ . The resulting exposures (fig. 2b) are then merged to a single HDR image using a conventional HDR merging algorithm [10].

**Multi-exposure prediction network** The backbone of our light intensity estimation is ICLight [73], a diffusion-based model fine-tuned for relighting, since it demonstrated strong performance in understanding lighting conditions. We further fine-tune it for HDR estimation as shown in fig. 2a. To do so, the input image is encoded into latent space and concatenated with the initial noise. As in RGB $\leftrightarrow$ X [70], we employ text-based conditioning to tell the network whether it should output a darker  $I_{-2} = \mathcal{D}_-(I_0)$  (conditioning text: “dark”) or brighter  $I_{+2} = \mathcal{D}_+(I_0)$  (“bright”) exposure. The network accepts a LDR image in sRGB space (with  $\gamma = 2.2$  [12]), and is trained to produce a re-exposed version of the input, also in sRGB space. Exposure  $I_0$  is therefore simply the input image.

At inference time, the network can be applied recursively to the predicted exposures to further expand the dynamic range (*i.e.*,  $I_{+4} = \mathcal{D}_+(\mathcal{D}_+(I_0))$ ) as illustrated in fig. 2b. In practice, we repeat this process until images no longer contain (under- or over-)saturated pixels.

**HDR merging** We consider the output from our multi-exposure estimation as a sequence of exposure-bracketed images  $\{I_{-2n}, \dots, I_{+2m}\}$  [48], where  $n$  and  $m$  indicate the number of dark and bright exposures estimated by the net-

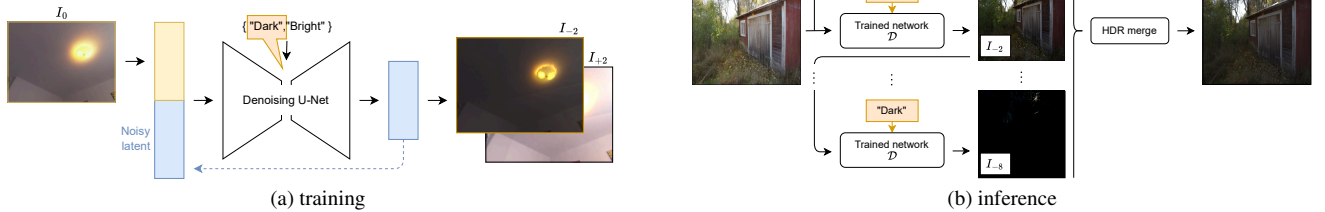


Figure 2. Overview of our HDR estimation pipeline. (a) We train a diffusion model to predict two exposures (brighter or darker) given an input image. (b) At inference time, we recursively apply the same network to obtain an exposure stack, which is subsequently merged to HDR.

work, respectively. We first linearize the images ( $\gamma = 2.2$ ), and then apply the Debevec HDR fusion method [10] to combine the sequence into a single HDR image. We adjust the weighting function to give a weight of 1 to pixels with intensity values in the range of  $[0.2, 0.8]$  in the original image  $I_0$ , ensuring unsaturated pixels are preserved as much as possible from  $I_0$ . This step prevents blurring due to the averaging of slightly different pixel values that can be generated by the diffusion model across exposures. The rest of the pixels are weighted using the original weighting function,  $w = -2|z - 0.5| + 1$ . This results in an image in linear, unbounded colorspace.

**360° prediction** Our method can also be naively applied to 360° panoramas by using a cube map representation and applying our method on each of the six faces independently. While this does not explicitly ensure consistency for light sources crossing the edges of the cube’s face, we observe that results obtained this way are usable and produce plausible lighting and reflections, effectively converting 360° into HDRI maps.

**Training data and implementation details** We employ a dataset of 12,611 HDR 360° panoramas to train our light intensity estimation model, containing a mix of publicly available [5, 45] and captured data. At training time, we project the spherical panorama to an image plane, using random parameters drawn according to the distributions shown in tab. 2. Note that images are first re-exposed using [49] such that the of the log-luma channel is 0.17 prior to applying the exposure augmentation from tab. 2. We also randomly apply a tone-mapping operator between gamma, Filmic, or Hybrid-Log-Gamma to ensure the model is robust to various camera functions. We normalize the output of the tonemapping operators to  $[-1, 1]$  to fit Stable Diffusion’s original training range. We obtain the prompts from each image using LLaVA [35].

Parameter	Distribution
Azimuth	$\mathcal{U}[0, 2\pi]$
Elevation	$\mathcal{U}[-\pi/2, \pi/2]$
Roll	$\mathcal{U}[-\pi/16, \pi/16]$
Vert. FoV	$\mathcal{U}[60^\circ, 120^\circ]$
Exposure	$2^e, e \sim \mathcal{U}[-8, 4]$

Table 2. Sampling parameters to generate training data for our HDR light intensity estimation network. Here,  $\mathcal{U}[a, b]$  denotes a uniform distribution in the  $[a, b]$  interval.

Our captured data was acquired in static scenes using a Ricoh Theta Z1 with exposure bracketing of 10 captures spanning from 1s to 1/25000s to obtain unsaturated captures. The camera was set to  $f/2.1$ , ISO 80, and fixed 5000K white balance for all captures. We stitched the RAW stereo spherical captures using PTGui [42].

We initialize our Stable Diffusion 1.5 backbone [50] with the IC-Light [73] checkpoint and fine-tune it for 415k iterations. We employ an initial learning rate of  $10^{-5}$ . Training took 10 days on 8 A100 GPUs with 40GB of VRAM. We perform 20 diffusion steps at inference, which takes a total of approximately 40 seconds on an Nvidia Titan V GPU.

### 3.2. Gaussian Splat lighting representation

We utilize the 3D Gaussian Splatting framework (3DGS) [29] as our HDR lighting representation. This representation offers multiple benefits, establishing it as a superior option over other lighting representations, as detailed in tab. 1.

As illustrated in fig. 3, we first process each image in the set with our HDR extrapolation network (c.f. sec. 3.1) to obtain (linear) HDR images. Then, we apply the training process proposed by InstantSplat [14] to recover an HDR 3DGS representation of the scene (in linear space). To train the 3DGS, the following loss is used:

$$\ell = \ell_2(\log(y^* + 1), \log(y + 1)), \quad (1)$$

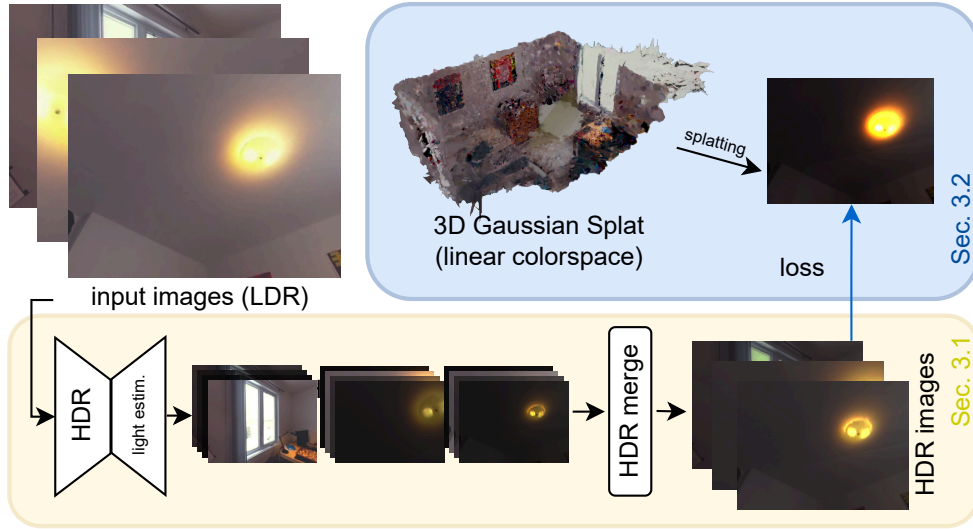


Figure 3. Overview of our 3D reconstruction pipeline. From a collection of LDR input images, we first convert them to HDR by using our HDR light intensity estimation network (bottom, see sec. 3.1). A 3D Gaussian Splatting (3DGS) representation is subsequently trained on the resulting HDR images (top).

where  $y$  and  $y^*$  are the predicted and ground truth HDR pixel values, respectively.

## 4. Evaluation

In this section, we first discuss the datasets used for evaluation, followed by an evaluation of our light source intensity estimation model against previous LDR-to-HDR methods. Lastly, we demonstrate that our 3D lighting framework better represents lighting conditions in natural scenes than previous work.

### 4.1. Data

To evaluate our light source intensity estimation model from sec. 3.1, we employ the following two datasets from the literature.

**Si-HDR [23]** is comprised of 195 captures, each composed of 5 RAW exposures, which are merged into HDR stacks. They also provide a reference LDR image for each capture, which is obtained by applying a custom CRF and adding realistic camera noise modeled from the Canon 5D Mark III. The dataset depicts various indoor and outdoor scenes with light sources and saturated highlights in the frame.

Analyzing the dataset reveals that 82 captures hold saturated pixels, even at the fastest shutter speed, an example of this is shown in fig. 4. While these captures allow for expanding the dynamic range of LDR images for purposes such as re-tonemapping, the saturated captures cannot faithfully represent the dynamic range of light sources. In our

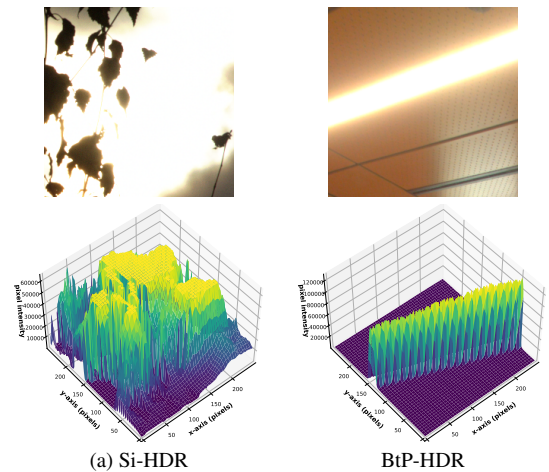


Figure 4. Comparison of images from the (a) Si-HDR [23] and (b) BtP-HDR [5] datasets. Image crops are shown on the top row, while the bottom row shows the corresponding plot of the luminance, showing of (a) a saturated sample from the Si-HDR dataset; and (b) an unsaturated sample from BtP-HDR. The large flat regions of maximum intensity in (a) correspond to saturated pixel values. the BtP-HDR dataset does not contain such saturation.

evaluation, we eliminate the saturated captures, which results in 113 HDR images.

**Beyond the Pixel [5] (BtP-HDR)** The unsaturated HDR dataset proposed for evaluation in [5] was expressly conceived to evaluate the presence of bright light sources in images. Contrarily to Si-HDR, the LDR reference image of this dataset is an actual capture from a camera, instead of a

Method	Si-HDR		BtP-HDR	
	MSE $\downarrow$	PSNR $\uparrow$	MSE $\downarrow$	PSNR $\uparrow$
LDR	0.0715	13.0605	0.0282	17.5467
HDRCNN	0.0246	23.6138	0.0060	30.6715
MaskHDR	0.0243	23.5503	0.0061	30.9510
SingleHDR	0.0178	24.0680	0.0092	23.6101
ExpandNet	0.0187	24.7158	0.0148	22.5799
Exposure Diff	0.0264	23.7384	0.0061	27.4963
Ours	0.0131	25.3895	0.0041	28.7022

Table 3. Quantitative evaluation of renderings lit by each method’s HDR image output. Results are color coded by **best**, **second** and **third best**.

simulated re-exposition from the HDR merged image. We dub this dataset BtP-HDR henceforth.

## 4.2. Light source estimation

We evaluate our novel light intensity estimation method (sec. 3.1) on the task of bright light source prediction. We first show qualitative results on the filtered Si-HDR dataset in fig. 5 and on the BtP-HDR dataset in fig. 6. The figures illustrate both the luminance of the generated HDR maps, as well as a render of a sphere on a plane lit by the color HDR map. Since these images are not full 360° environment maps, we project them onto a partial hemisphere of 90° field of view, and use this as light source for rendering. The camera, plane, and sphere are located at the origin, facing the camera. The glossy sphere has an albedo of 1 (pure white) and a roughness coefficient of 0. We make sure all HDR images used as lighting are exposed the same way by aligning the averages of pixels with intensity between 0.2 and 0.8 with the ground truth. Observe how the predictions made by our method more closely match the ground truth, especially when bright light sources generate hard cast shadows on the plane and bright specularities on the sphere.

To further assess the accuracy of our method, we compute quantitative image comparison metrics (MSE and PSNR) on the renders compared to the ground truth in tab. 3. We observe that our method significantly outperforms existing methods in terms of both MSE and PSNR on the filtered Si-HDR dataset. On the BtP-HDR dataset, our method provides the best MSE score while offering a competitive PSNR value. We attribute this lower score to the fact that BtP-HDR features indoor scenes that tend to have a lower dynamic range than outdoor environments. Consequently, techniques like HDRCNN and MaskHDR perform well in areas that are slightly above saturation.

## 4.3. 3D lighting representation

The approach that is most closely related to ours is that of PanoHDR-NeRF [19], who train a NeRF-based implicit

Scene	PanoHDR-NeRF		Ours	
	MSE $\downarrow$	PSNR $\uparrow$	MSE $\downarrow$	PSNR $\uparrow$
Chess room	0.0247	17.5010	0.0053	25.9313
Small class	0.1097	9.7872	0.0061	23.1244

Table 4. Quantitative evaluation of renderings lit by novel views of PanoHDR-NeRF [19] and Ours, as compared to the captured HDR ground truth panoramas provided in [19]. Our method achieves the best scores on both scenes for all metrics.

representation on images that have been converted to HDR using the LANet [69] LDR-to-HDR architecture. They also provide a dataset of interior scenes captured with a 360° camera, in which a few (between 8–10) ground truth HDR panoramas were captured using exposure bracketing.

We therefore compare our HDR Gaussian Splatting representation to PanoHDR-NeRF on two scenes from their dataset and show the quantitative results in tab. 4. These metrics were computed by first rendering a synthetic scene (similar to sec. 4.2), lit by each method’s prediction, and compared to the ground truth. The table shows that our method significantly outperforms the baseline. We note that the results they report in their paper also include a version of LANet fine-tuned on a small dataset of HDR images captured by the same camera that was used to capture the ground truth—we use the “vanilla” model to avoid unfairly advantaging the method, and assume that no method has knowledge of the actual camera used to capture the data.

## 5. Application: virtual object insertion

The 3DGS representation is inherently 3D, allowing for near-field lighting effects out-of-the-box. It is possible to composite virtual objects directly in this representation, as shown in fig. 1. We obtain these results by importing our 3DGS representation directly in Blender [8], setting the Gaussians as emitters, and rendering the scene using the Cycles physically-based renderer. The inserted objects are automatically lit with near-field lighting effects, without manual intervention or custom lights in the scene.

## 6. Conclusion

**Limitations** Despite encouraging results, GASLIGHT suffers from some limitations. First, each Gaussian in the 3DGS representation is effectively considered to be a light source (*e.g.*, when rendering, see sec. 5. This precludes the simulation of more complex lighting effects, such as interreflections or scattering. Here, it is likely that new raytracing-based approaches [40] could help. Second, our HDR light intensity estimation network is not trained to achieve multi-view consistency: it is therefore possible that different content is extrapolated for two nearby views.

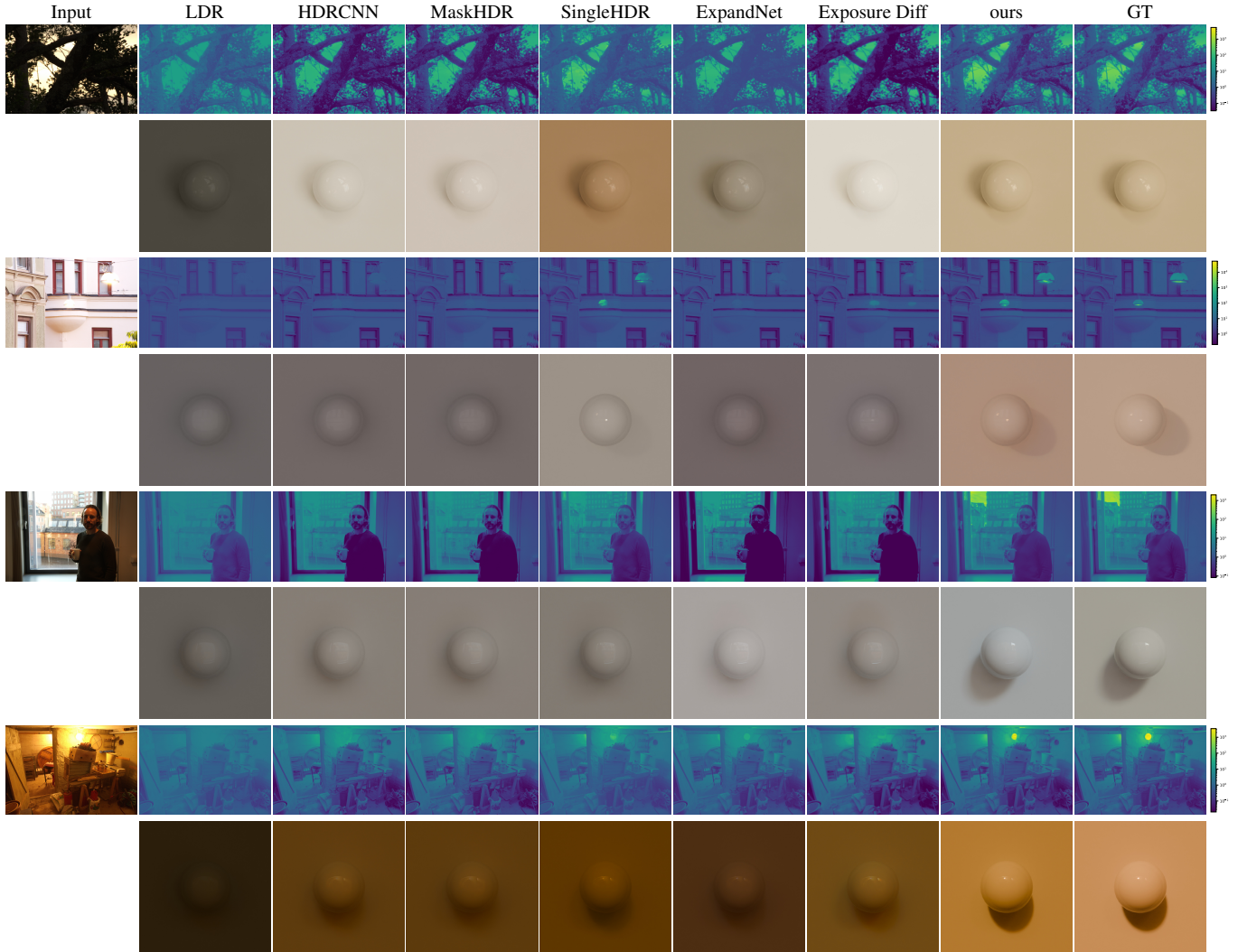


Figure 5. Qualitative evaluation on the filtered Si-HDR dataset [23]. From an LDR image (left), we compare the luminance of each method’s predicted HDR (even rows) and the rendering of a glossy sphere illuminated by the prediction (odd rows). Our approach more accurately estimates light intensity, producing renders similar to those rendered using the ground truth HDR image.

While the spherical harmonics in the 3DGS representation alleviates for this somewhat and can realistically blend inconsistent predictions, future work could enforce such consistency, for example through score distillation sampling [46]. We also note that, as opposed to most lighting estimation methods that predict light sources outside the field of view of the image, we only recover the lighting for visible parts of the scene. Combining our method with view extrapolation approaches (*e.g.*, [7, 43]) is a promising future direction. Finally, our current implementation, which relies on InstantSplat [14] does not scale well to large scenes. This is somewhat orthogonal to our goal of capturing lighting—we are hopeful that new developments (*e.g.*, [30]) could help alleviate this.

We present GASLIGHT, a novel Gaussian Splatting-

based HDR Lighting representation. The core of our method is a diffusion-based LDR-to-HDR model that uses its priors of natural images to expand the dynamic ranges of LDR images to unsaturated, even on bright light sources such as the sun. We further fit a 3DGS model on the predicted HDR images, which results in a light representation that can model spatially-varying effects, achieves high frequency reflections and hard cast shadows, and can readily be integrated in existing rendering engines.

**Acknowledgements** This research was supported by Sentinel North, NSERC grant RGPIN 2020-04799, and the Digital Research Alliance Canada.

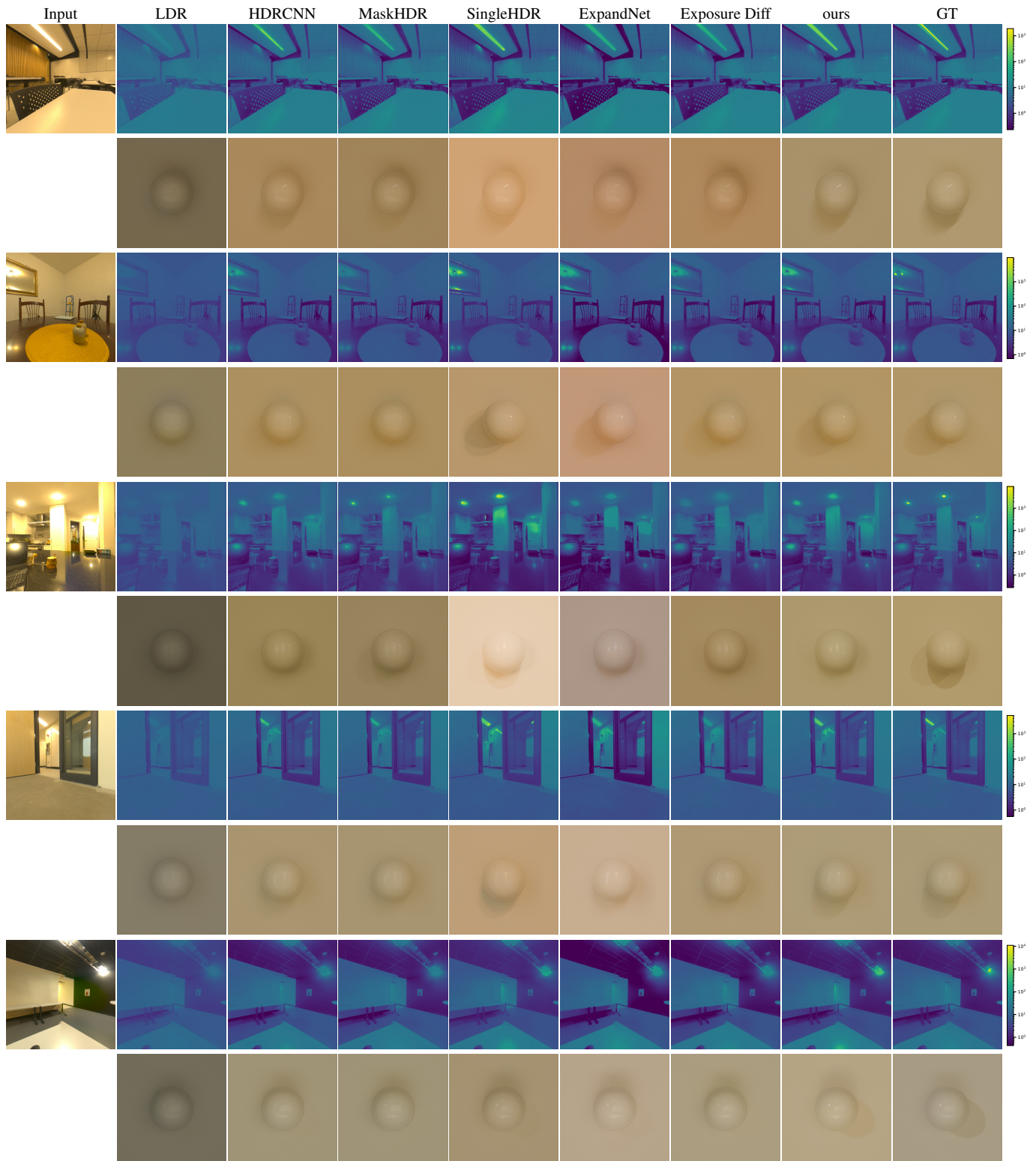


Figure 6. Qualitative evaluation on the BtP-HDR dataset [5]. From an LDR image (left), we compare the luminance of each method’s predicted HDR (even rows) and the rendering of a glossy sphere illuminated by the prediction (odd rows). Our approach more accurately estimates light intensity, producing renders similar to those rendered using the ground truth HDR image.

## References

- [1] Francesco Banterle, Patrick Ledda, Kurt Debattista, and Alan Chalmers. Inverse tone mapping. In *Proceedings of the 4th international conference on Computer graphics and interactive techniques in Australasia and Southeast Asia*, pages 349–356, 2006. 2
- [2] Axel Barroso-Laguna, Sowmya Munukutla, Victor Prisacariu, and Eric Brachmann. Matching 2d images in 3d: Metric relative pose from metric correspondences. In *IEEE/CVF Conf. Comput. Vis. Pattern Recog.*, 2024. 3
- [3] Mojtaba Bemana, Thomas Leimkühler, Karol Myszkowski, Hans-Peter Seidel, and Tobias Ritschel. Exposure diffusion: Hdr image generation by consistent ldr denoising. *arXiv preprint arXiv:2405.14304*, 2024. 2
- [4] James F Blinn and Martin E Newell. Texture and reflection in computer generated images. *Communications of the ACM*, 19(10):542–547, 1976. 3
- [5] Christophe Bolduc, Justine Giroux, Marc Hébert, Claude Demers, and Jean-François Lalonde. Beyond the pixel: a photometrically calibrated HDR dataset for luminance and color prediction. In *IEEE/CVF Int. Conf. Comput. Vis.*, 2023. 4, 5, 8
- [6] Yuanhao Cai, Zihao Xiao, Yixun Liang, Minghan Qin, Yulun Zhang, Xiaokang Yang, Yaoyao Liu, and Alan L Yuille. HDR-GS: Efficient high dynamic range novel view synthesis at 1000x speed via gaussian splatting. In *Adv. Neural Inform. Process. Syst.*, pages 68453–68471, 2025. 2
- [7] Jaeyoung Chung, Suyoung Lee, Hyeongjin Nam, Jaerin Lee, and Kyoung Mu Lee. Luciddreamer: Domain-free generation of 3d gaussian splatting scenes. *arXiv preprint arXiv:2311.13384*, 2023. 7
- [8] Blender Online Community. *Blender - a 3D modelling and rendering package*. Blender Foundation, Stichting Blender Foundation, Amsterdam, 2018. 6
- [9] Mohammad Reza Karimi Dastjerdi, Jonathan Eisenmann, Yannick Hold-Geoffroy, and Jean-François Lalonde. Everlight: Indoor-outdoor editable HDR lighting estimation. In *IEEE/CVF Int. Conf. Comput. Vis.*, 2023. 2, 3
- [10] Paul E. Debevec and Jitendra Malik. Recovering high dynamic range radiance maps from photographs. In *Proceedings of the 24th Annual Conference on Computer Graphics and Interactive Techniques*, page 369–378, 1997. 1, 2, 3, 4
- [11] Daniel DeTone, Tomasz Malisiewicz, and Andrew Rabynovich. Superpoint: Self-supervised interest point detection and description. In *IEEE Conf. Comput. Vis. Pattern Recog. Worksh.*, 2018. 3
- [12] Gabriel Eilertsen, Joel Kronander, Gyorgy Denes, Rafal Mantiuk, and Jonas Unger. Hdr image reconstruction from a single exposure using deep cnns. *ACM Trans. Graph.*, 36(6), 2017. 1, 2, 3
- [13] Yuki Endo, Yoshihiro Kanamori, and Jun Mitani. Deep reverse tone mapping. *ACM Trans. Graph.*, 36(6):1–10, 2017. 2
- [14] Zhiwen Fan, Wenyan Cong, Kairun Wen, Kevin Wang, Jian Zhang, Xinghao Ding, Danfei Xu, Boris Ivanovic, Marco Pavone, Georgios Pavlakos, Zhangyang Wang, and Yue Wang. Instantsplat: Unbounded sparse-view pose-free gaussian splatting in 40 seconds, 2024. 4, 7
- [15] James D Foley. *Computer graphics: principles and practice*. Addison-Wesley Professional, 1996. 2
- [16] Marc-André Gardner, Kalyan Sunkavalli, Ersin Yumer, Xiaohui Shen, Emiliano Gambaretto, Christian Gagné, and Jean-François Lalonde. Learning to predict indoor illumination from a single image. *ACM Trans. Graph.*, 2017. 2, 3
- [17] Marc-André Gardner, Yannick Hold-Geoffroy, Kalyan Sunkavalli, Christian Gagné, and Jean-François Lalonde. Deep parametric indoor lighting estimation. In *IEEE/CVF Int. Conf. Comput. Vis.*, 2019. 1, 3
- [18] Mathieu Garon, Kalyan Sunkavalli, Sunil Hadap, Nathan Carr, and Jean-François Lalonde. Fast spatially-varying indoor lighting estimation. In *IEEE/CVF Conf. Comput. Vis. Pattern Recog.*, 2019. 1, 3
- [19] Pulkit Gera, Mohammad Reza Karimi Dastjerdi, Charles Renaud, PJ Narayanan, and Jean-François Lalonde. Casual indoor hdr radiance capture from omnidirectional images. *Brit. Mach. Vis. Conf.*, 33, 2022. 2, 3, 6
- [20] Michaël Gharbi, Jiawen Chen, Jonathan T Barron, Samuel W Hasinoff, and Frédo Durand. Deep bilateral learning for real-time image enhancement. *ACM Trans. Graph.*, 36(4):1–12, 2017. 1
- [21] Robin Green. Spherical harmonic lighting: The gritty details. In *Archives of the game developers conference*, page 4, 2003. 3
- [22] David Griffiths, Tobias Ritschel, and Julien Philip. Outcast: Outdoor single-image relighting with cast shadows. In *Comput. Graph. Forum*, pages 179–193. Wiley Online Library, 2022. 3
- [23] Param Hanji, Rafal Mantiuk, Gabriel Eilertsen, Saghi Hajisharif, and Jonas Unger. Comparison of single image HDR reconstruction methods—the caveats of quality assessment. In *ACM SIGGRAPH Conf.*, 2022. 5, 7
- [24] Samuel W Hasinoff, Dillon Sharlet, Ryan Geiss, Andrew Adams, Jonathan T Barron, Florian Kainz, Jiawen Chen, and Marc Levoy. Burst photography for high dynamic range and low-light imaging on mobile cameras. *ACM Trans. Graph.*, 35(6):1–12, 2016. 1
- [25] Landis Hayden. Production-ready global illumination. In *Siggraph 2002*, pages 93–95, 2002. 2
- [26] Yannick Hold-Geoffroy, Akshaya Athawale, and Jean-François Lalonde. Deep sky modeling for single image outdoor lighting estimation. In *IEEE/CVF Conf. Comput. Vis. Pattern Recog.*, 2019. 3
- [27] Xin Huang, Qi Zhang, Ying Feng, Hongdong Li, Xuan Wang, and Qing Wang. HDR-NeRF: High dynamic range neural radiance fields. In *IEEE/CVF Conf. Comput. Vis. Pattern Recog.*, 2022. 2
- [28] Kim Jun-Seong, Kim Yu-Ji, Moon Ye-Bin, and Tae-Hyun Oh. HDR-plenoxels: Self-calibrating high dynamic range radiance fields. In *Eur. Conf. Comput. Vis.*, 2022. 2
- [29] Bernhard Kerbl, Georgios Kopanas, Thomas Leimkühler, and George Drettakis. 3d gaussian splatting for real-time radiance field rendering. *ACM Trans. Graph.*, 42(4):139–1, 2023. 2, 4

- [30] Bernhard Kerbl, Andreas Meuleman, Georgios Kopanas, Michael Wimmer, Alexandre Lanvin, and George Drettakis. A hierarchical 3D gaussian representation for real-time rendering of very large datasets. *ACM Trans. Graph.*, 43(4): 1–15, 2024. 7
- [31] Vincent Leroy, Johann Cabon, and Jerome Revaud. Grounding image matching in 3d with mast3r, 2024. 3
- [32] Zhengqin Li, Mohammad Shafiei, Ravi Ramamoorthi, Kalyan Sunkavalli, and Manmohan Chandraker. Inverse rendering for complex indoor scenes: Shape, spatially-varying lighting and svbrdf from a single image. In *IEEE/CVF Conf. Comput. Vis. Pattern Recog.*, 2020. 1
- [33] Zhengqin Li, Li Yu, Mikhail Okunev, Manmohan Chandraker, and Zhao Dong. Spatiotemporally consistent HDR indoor lighting estimation. *ACM Trans. Graph.*, 42(3):1–15, 2023. 1, 3
- [34] Jingwang Ling, Ruihan Yu, Feng Xu, Chun Du, and Shuang Zhao. Nerf as a non-distant environment emitter in physics-based inverse rendering. In *ACM SIGGRAPH Conf.*, pages 1–12, 2024. 3
- [35] Haotian Liu, Chunyuan Li, Qingyang Wu, and Yong Jae Lee. Visual instruction tuning. In *NeurIPS*, 2023. 4
- [36] Yu-Lun Liu, Wei-Sheng Lai, Yu-Sheng Chen, Yi-Lung Kao, Ming-Hsuan Yang, Yung-Yu Chuang, and Jia-Bin Huang. Single-image hdr reconstruction by learning to reverse the camera pipeline. In *IEEE/CVF Conf. Comput. Vis. Pattern Recog.*, 2020. 1, 2
- [37] Demetris Marnerides, Thomas Bashford-Rogers, Jonathan Hatchett, and Kurt Debattista. Expandnet: A deep convolutional neural network for high dynamic range expansion from low dynamic range content. In *Comput. Graph. Forum*, pages 37–49. Wiley Online Library, 2018. 2
- [38] Ben Mildenhall, Pratul P Srinivasan, Matthew Tancik, Jonathan T Barron, Ravi Ramamoorthi, and Ren Ng. Nerf: Representing scenes as neural radiance fields for view synthesis. *Communications of the ACM*, 65(1):99–106, 2021. 2
- [39] Ben Mildenhall, Peter Hedman, Ricardo Martin-Brualla, Pratul P Srinivasan, and Jonathan T Barron. Nerf in the dark: High dynamic range view synthesis from noisy raw images. In *IEEE/CVF Conf. Comput. Vis. Pattern Recog.*, 2022. 2
- [40] Nicolas Moenne-Loccoz, Ashkan Mirzaei, Or Perel, Riccardo de Lutio, Janick Martinez Esturo, Gavriel State, Sanja Fidler, Nicholas Sharp, and Zan Gojcic. 3d gaussian ray tracing: Fast tracing of particle scenes. *ACM Trans. Graph.*, 43(6):1–19, 2024. 6
- [41] Shree K Nayar and Tomoo Mitsunaga. High dynamic range imaging: Spatially varying pixel exposures. In *Proceedings IEEE Conference on Computer Vision and Pattern Recognition. CVPR 2000 (Cat. No. PR00662)*, pages 472–479. IEEE, 2000. 1
- [42] New House Internet Services B.V., Rotterdam, The Netherlands. Ptgui. 4
- [43] Avinash Paliwal, Xilong Zhou, Andrii Tsarov, and Nima Khademi Kalantari. Panodreamer: 3d panorama synthesis from a single image. *arXiv preprint arXiv:2412.04827*, 2024. 7
- [44] Pakkapon Phongthawee, Worameth Chinchuthakun, Non-taphat Sinsunthithet, Varun Jampani, Amit Raj, Pramook Khungurn, and Supasorn Suwajanakorn. Diffusionlight: Light probes for free by painting a chrome ball. In *IEEE/CVF Conf. Comput. Vis. Pattern Recog.*, 2024. 2, 3
- [45] PolyHaven. Poly haven: The public 3d asset library. 2025. 4
- [46] Ben Poole, Ajay Jain, Jonathan T Barron, and Ben Mildenhall. Dreamfusion: Text-to-3d using 2d diffusion. *arXiv preprint arXiv:2209.14988*, 2022. 7
- [47] Ravi Ramamoorthi and Pat Hanrahan. An efficient representation for irradiance environment maps. In *Proceedings of the 28th annual conference on Computer graphics and interactive techniques*, pages 497–500, 2001. 3
- [48] Erik Reinhard. High dynamic range imaging. In *Computer Vision: A Reference Guide*, pages 1–6. Springer, 2020. 3
- [49] Erik Reinhard, Michael Stark, Peter Shirley, and James Ferwerda. Photographic tone reproduction for digital images. *ACM Trans. Graph.*, 21(3):267–276, 2002. 4
- [50] Robin Rombach, Andreas Blattmann, Dominik Lorenz, Patrick Esser, and Björn Ommer. High-resolution image synthesis with latent diffusion models. In *IEEE/CVF Conf. Comput. Vis. Pattern Recog.*, 2022. 2, 4
- [51] Paul-Edouard Sarlin, Daniel DeTone, Tomasz Malisiewicz, and Andrew Rabinovich. Superglue: Learning feature matching with graph neural networks. In *IEEE/CVF Conf. Comput. Vis. Pattern Recog.*, 2020. 3
- [52] Johannes Lutz Schönberger and Jan-Michael Frahm. Structure-from-motion revisited. In *IEEE/CVF Conf. Comput. Vis. Pattern Recog.*, 2016. 3
- [53] Johannes Lutz Schönberger, Enliang Zheng, Marc Pollefeys, and Jan-Michael Frahm. Pixelwise view selection for unstructured multi-view stereo. In *Eur. Conf. Comput. Vis.*, 2016. 3
- [54] Peter-Pike Sloan, Jan Kautz, and John Snyder. Precomputed radiance transfer for real-time rendering in dynamic, low-frequency lighting environments. In *Seminal Graphics Papers: Pushing the Boundaries, Volume 2*, pages 339–348. 2023. 3
- [55] Gowri Somanath and Daniel Kurz. HDR environment map estimation for real-time augmented reality. In *IEEE/CVF Conf. Comput. Vis. Pattern Recog.*, 2021. 2, 3
- [56] Shuran Song and Thomas Funkhouser. Neural illumination: Lighting prediction for indoor environments. In *IEEE/CVF Conf. Comput. Vis. Pattern Recog.*, 2019. 2, 3
- [57] Pratul P Srinivasan, Ben Mildenhall, Matthew Tancik, Jonathan T Barron, Richard Tucker, and Noah Snavely. Lighthouse: Predicting lighting volumes for spatially-coherent illumination. In *IEEE/CVF Conf. Comput. Vis. Pattern Recog.*, 2020. 1, 3
- [58] Jessi Stumpfel, Andrew Jones, Andreas Wenger, Chris Tchou, Tim Hawkins, and Paul Debevec. Direct HDR capture of the sun and sky. In *ACM SIGGRAPH 2006 Courses*, pages 5–es. 2006. 1
- [59] Bill Triggs, Philip F McLauchlan, Richard I Hartley, and Andrew W Fitzgibbon. Bundle adjustment—a modern synthesis. In *Int. Worksh. Vis. Alg.* Springer, 2000. 3

- [60] Chao Wang, Ana Serrano, Xingang Pan, Bin Chen, Karol Myszkowski, Hans-Peter Seidel, Christian Theobalt, and Thomas Leimkühler. Glowgan: Unsupervised learning of hdr images from ldr images in the wild. In *IEEE/CVF Int. Conf. Comput. Vis.*, 2023. 2
- [61] Chao Wang, Krzysztof Wolski, Bernhard Kerbl, Ana Serrano, Mojtaba Bermana, Hans-Peter Seidel, Karol Myszkowski, and Thomas Leimkühler. Cinematic gaussians: Real-time HDR radiance fields with depth of field. In *Comput. Graph. Forum*, page e15214. Wiley Online Library, 2024. 3
- [62] Chao Wang, Zhihao Xia, Thomas Leimkühler, Karol Myszkowski, and Xuaner Zhang. Lediff: Latent exposure diffusion for hdr generation. *arXiv preprint arXiv:2412.14456*, 2024. 1, 2
- [63] Fangjinhua Wang, Qingtian Zhu, Di Chang, Quankai Gao, Junlin Han, Tong Zhang, Richard Hartley, and Marc Pollefeys. Learning-based multi-view stereo: a survey. *arXiv preprint arXiv:2408.15235*, 2024. 3
- [64] Shuzhe Wang, Vincent Leroy, Yohann Cabon, Boris Chidlovskii, and Jerome Revaud. Dust3r: Geometric 3d vision made easy. In *IEEE/CVF Conf. Comput. Vis. Pattern Recog.*, 2024. 3
- [65] Yuehao Wang, Chaoyi Wang, Bingchen Gong, and Tianfan Xue. Bilateral guided radiance field processing. *ACM Trans. Graph.*, 43(4):1–13, 2024. 2
- [66] Zian Wang, Jonah Philion, Sanja Fidler, and Jan Kautz. Learning indoor inverse rendering with 3D spatially-varying lighting. In *IEEE/CVF Conf. Comput. Vis. Pattern Recog.*, 2021. 1
- [67] Zian Wang, Tianchang Shen, Jun Gao, Shengyu Huang, Jacob Munkberg, Jon Hasselgren, Zan Gojcic, Wenzheng Chen, and Sanja Fidler. Neural fields meet explicit geometric representations for inverse rendering of urban scenes. In *IEEE/CVF Conf. Comput. Vis. Pattern Recog.*, 2023. 3
- [68] Guanjun Wu, Taoran Yi, Jiemin Fang, Wenyu Liu, and Xingang Wang. Fast high dynamic range radiance fields for dynamic scenes. In *Int. Conf. 3D Vis.*, 2024. 2
- [69] Hanning Yu, Wentao Liu, Chengjiang Long, Bo Dong, Qin Zou, and Chunxia Xiao. Luminance attentive networks for hdr image and panorama reconstruction. In *Comput. Graph. Forum*, pages 181–192. Wiley Online Library, 2021. 1, 2, 6
- [70] Zheng Zeng, Valentin Deschaintre, Iliyan Georgiev, Yannick Hold-Geoffroy, Yiwei Hu, Fujun Luan, Ling-Qi Yan, and Miloš Hašan. RGB  $\leftrightarrow$  X: Image decomposition and synthesis using material-and lighting-aware diffusion models. In *ACM SIGGRAPH Conf.*, 2024. 3
- [71] Fangneng Zhan, Changgong Zhang, Yingchen Yu, Yuan Chang, Shijian Lu, Feiying Ma, and Xuansong Xie. Emlight: Lighting estimation via spherical distribution approximation. In *Assoc. Adv. of Art. Int.*, 2021. 3
- [72] Jinsong Zhang and Jean-François Lalonde. Learning high dynamic range from outdoor panoramas. In *IEEE/CVF Int. Conf. Comput. Vis.*, 2017. 2
- [73] Lvmin Zhang, Anyi Rao, and Maneesh Agrawala. Scaling in-the-wild training for diffusion-based illumination harmonization and editing by imposing consistent light transport. In *Int. Conf. Learn. Represent.*, 2025. 3, 4